ISSN 1674-1056
http://cpb.iphy.ac.cn
http://iopscience.iop.org/cpb
中国物理 B
Chinese Physics
中国物理
Chinese Physics B

Tunability of Fano resonance in cylindrical core-shell nanorods

Ben-Li Wang(王本立)

Citation: Chin. Phys. B . 2020, 29(4): 045202 . **doi:** 10.1088/1674-1056/ab75d1
Journal homepage: http://cpb.iphy.ac.cn; http://iopscience.iop.org/cpb

What follows is a list of articles you may be interested in

Influence of vibration on spatiotemporal structure of the pattern in dielectric barrier discharge

Rong Han(韩蓉), Li-Fang Dong(董丽芳), Jia-Yu Huang(黄加玉), Hao-Yang Sun(孙浩洋), Bin-Bin Liu(刘彬彬), Yan-Lin Mi(米彦霖)

Chin. Phys. B . 2019, 28(7): 075204 . **doi:** 10.1088/1674-1056/28/7/075204

Characteristic plume morphologies of atmospheric Ar and He plasma jets excited by a pulsed microwave hairpin resonator

Zhao-Quan Chen(陈兆权), Ben-Kuan Zhou(周本宽), Huang Zhang(张煌), Ling-Li Hong(洪伶俐), Chang-Lin Zou(邹长林), Ping Li(李平), Wei-Dong Zhao(赵卫东), Xiao-Dong Liu(刘晓东), Olga Stepanova, A A Kudryavtsev

Chin. Phys. B . 2018, 27(5): 055202 . **doi:** 10.1088/1674-1056/27/5/055202

Drift vortices in inhomogeneous collisional dusty magnetoplasma

Jian-Rong Yang(杨建荣), Kui Lv(吕岿), Lei Xu(许磊), Jie-Jian Mao(毛杰键), Xi-Zhong Liu(刘希忠), Ping Liu(刘萍)

Chin. Phys. B . 2017, 26(6): 065202 . **doi:** 10.1088/1674-1056/26/6/065202

Nonlinear parametric interactions in ion-implanted semiconductor plasmas having strain-dependent dielectric constants

N Yadav, S Ghosh, P S Malviya

Chin. Phys. B . 2017, 26(1): 015203 . **doi:** 10.1088/1674-1056/26/1/015203

Dust acoustic waves in collisional uniform dense magnetoplasma

Jian-Rong Yang(杨建荣), Ting Xu(徐婷), Jie-Jian Mao(毛杰键), Ping Liu(刘萍), Xi-Zhong Liu(刘希忠)

Chin. Phys. B . 2017, 26(1): 015202 . **doi:** 10.1088/1674-1056/26/1/015202

Tunability of Fano resonance in cylindrical core–shell nanorods*

Ben-Li Wang(王本立)†

College of Mathematics and Physics, Beijing University of Chemical Technology, Beijing 100029, *China*

(Received 17 December 2019; revised manuscript received 22 January 2020; accepted manuscript online 13 February 2020)

The optical properties of cylindrical core–shell nanorods (CCSNs) are theoretically investigated in this paper. The results show that Fano resonance can be generated in CCSNs, and the wavelength and the intensity at Fano dip can be tuned respectively by adjusting the field coupling of cavity mode inside and near field on gold surface. The high tuning sensitivity which is about 400 nm per refractive-index unit can be obtained, and an easy-to-realize tunable parameter is also proposed. A two-oscillator model is also introduced to describe the generation of Fano resonance in CCSNs, and the results from this model are in good agreement with theoretical results. The CCSNs investigated in this work may have promising applications in optical devices.

Keywords: Fano resonance, tunability, local surface plasmon resonance, optical devices

PACS: 52.35.Mw, 41.20.Jb, 52.25.Tx **DOI:** 10.1088/1674-1056/ab75d1

1. Introduction

Fano resonance, originated from atomic physics,[1] has received great interest of researchers in many fields, such as plasmonics,[2–4] with the development of nanotechnology. Like it in atomic physics, the emergence of Fano resonance can be attributed to the coupling of broad resonance and narrow resonance supported in plasmonic systems.[5,6] Various kinds of plasmonic structures have been explored to achieve Fano resonance,[7–13] and some theoretical models were introduced to explain this optical phenomenon.[14–16] The potential applications of Fano resonance, such as optical sensors,[17,18] and nonlinear optical effects enhancement were also investigated extensively.[19] However, noble metals which are often the vital elements of plasmonic structures owe losses at optical frequencies.[20] Thus, the generation of Fano resonance in the coupled dielectric nanoparticles was also studied.[21]

The local surface plasmon resonance (LSPR) supported by many plasmonic structures is very sensitive to the geometry of metallic nanoparticle and environment.[22,23] Therefore, it is entirely feasible to tune the Fano resonance in plasmonic systems by using the LSPR's features previously described.[24,25] Although there were some researches on the tunability of Fano resonance,[26–29] they mainly focused on the spherical structures and resonance position adjustment. The tunability of the intensity of Fano resonance has been rarely studied, but this characteristic is also important and may be used to design optical nano-logical elements.

In this work, the optical extinction spectra of cylindrical core–shell nanorods (CCSNs) are theoretically investigated by using the finite-difference time-domain (FDTD) method. The Fano resonances are found in the CCSN structures based on the calculated results. We also find that the position of Fano resonance can be easily tuned by changing the refractive index of the dielectric core, and it can also be adjusted by varying the height of CCSNs. Moreover, the polarization-dependence is also investigated in this work, because it is easy to control the polarization of incident light in experiment. More importantly, it shows that the intensity of Fano resonance indeed can be controlled and tuned by the polarization of incident light. Our work can conduce to the potential applications of CCSNs in optical nano-device design and nonlinear optics.[17–19]

2. Theoretical model

The CCSN is a cylindrical dielectric nanorod coated by thin gold film. The geometry of the CCSN is shown in Fig. 1. The yellow part denotes the coated thin gold film, and the coordinate system is also presented there. We can see that the axial direction of the CCSN is along the x direction. The incident light propagates along the z direction, and the polarization is along the CCSN axis firstly.

The extinction spectra of CCSNs are calculated by the FDTD method. Then the Fano resonance can be analyzed by extinction spectra and field distribution. By changing the refractive index of the dielectric core, the Fano resonance can be tuned. The dependence of Fano resonance on the polarization of the incident light is also explored by extinction spectra. In the end, a two-oscillator model is introduced to reproduce the Fano resonance in the CCSN. It is an extension of the classical two-oscillator model[11] and the motion of the two oscillators can be described by the following two equations:

$$\ddot{x}_1(t)+\gamma_1\dot{x}_1(t)+\omega_1^2x_1(t)-\Omega_{12}^2x_2(t)=F\,\mathrm{e}^{-\mathrm{i}\omega t}\cos(\theta), \quad (1)$$

$$\ddot{x}_2(t)+\gamma_2\dot{x}_2(t)+\omega_2^2x_2(t)-\Omega_{12}^2x_1(t)=0. \quad (2)$$

*Project supported by the National Natural Science Foundation of China (Grant No. 11647021).

†Corresponding author. E-mail: wangbenli@mail.buct.edu.cn

© 2020 Chinese Physical Society and IOP Publishing Ltd

The hybridized modes of CCSNs are modeled as the two interacting oscillators with resonance frequencies ω_1 and ω_2 respectively. The two oscillators are coupled through the coefficient Ω_{12}. The oscillator 1 is driven by a harmonic force $F(t) = F\,\mathrm{e}^{-\mathrm{i}\omega t}\cos(\theta)$, where θ is the polarization angle of the incident light. x_1 and x_2 denote the displacements of oscillators 1 and 2 from their equilibrium position respectively. The coupling of the modes in CCSNs is similar to that of the two oscillators.

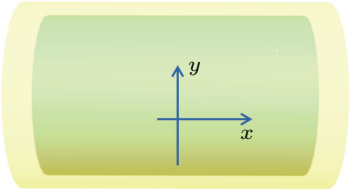


Fig. 1. Schematic diagram of core–shell cylindrical nanorod structure, where yellow part denotes coated gold thin film on dielectric core, and axial direction of the nanorod is along x.

3. Results and discussion

We start with examining the extinction spectrum of CCSNs. The extinction cross section is obtained by the FDTD simulations. First, the height and radius of the core of CCSN are fixed at 76 nm and 30 nm, respectively. The coating gold film along the axial direction is kept at 7 nm, and at 5 nm along the radial direction. The incident light is polarized along the x direction (axial direction). The refractive index of core is changed from 1.1 to 1.6, in steps of 0.1. The results for the CCSNs with different cores are presented in Figs. 2(a)–2(e). It shows that the Fano resonance induced in the CCSN with the low refractive index (such as $n = 1.1$ and 1.2 shown in Figs. 2(a) and 2(b)) core is too weak to be noticed. There is a distinct Fano resonance around 750 nm in the extinction spectrum of the CCSN with $n = 1.3$ shown in Fig. 2(c).

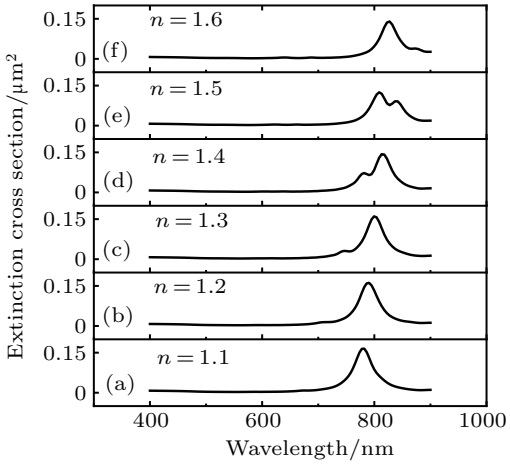


Fig. 2. Calculated extinction cross sections *versus* wavelength for core–shell nanorods with different cores. Height and radius of cores are fixed at 76 nm and 30 nm, respectively. Thickness of gold shell along axis direction is kept at 7 nm, and along radial direction at 5 nm. Refractive index of the core increases from (a) 1.1 to (b) 1.2 to (c) 1.3, and (d) 1.6 in steps of 0.1.

It can also be seen that as the refractive index of core increases from 1.3 to 1.6, the Fano resonance changes from about 750 nm to 870 nm. It can be concluded that the tuning sensitivity can reach about 400 nm per refractive-index unit. This high sensitivity makes it possess promising applications in chemical sensors or biosensors. Besides, it can be noticed that as the refractive index of the core increases, the intensity of Fano resonance is changing. However, the relationship between the intensity of Fano resonance and the refractive index of the core in CCSNs is not linear.

The optical response of metallic core–shell nanostructures can be seen as the interaction between modes supported by elementary shapes.[30] The CCSN can be seen as a combination of a gold nanorod and a gold cavity. The electric field intensity for the gold nanorod and for the cavity with the same structural parameters are calculated respectively. The normalized electric field intensities for the two elementary shapes are shown in Fig. 3, where the black line is for the nanorod, and the red line is for the cavity. It can be seen that a broad mode supported by the cavity and a narrow mode supported by the nanorod are existent. Therefore, the Fano resonance can be generated by tuning the coupling the two modes. In order to further understand the origin of the Fano resonance existing in CCSNs, the electric field intensity distributions are also calculated. Here the parameters of the CCSN are set to be the values the same as those discussed previously, and the refractive index of core is fixed at 1.3, where we start to clearly observe the Fano resonance discussed previously. The field intensity distributions are shown in Fig. 4. The wavelengths of the electric field are chosen for three different conditions. The first one is for the peak of Fano resonance with $\lambda = 745$ nm as shown in Fig. 4(a), the second one is for the dip of Fano resonance with $\lambda = 757$ nm as shown in Fig. 4(b), and the last one is for peak of the local surface plasmon resonance (LSPR) with $\lambda = 799$ nm as shown in Fig. 4(c). Concerning the peak of Fano resonance, which is located at 745 nm, we can observe an obvious field coupling between the cavity mode inside the dielectric core and the enhanced field near the gold surface in Fig. 4(a). Therefore, a Fano resonance peak occurs in the extinction spectrum as a result of field coupling. Concerning the dip of Fano resonance, which is located at 757 nm, we can still observe a weak field coupling in Fig. 4(b). It can be noticed that the field coupling occurs when the field passes through the thin gold shell which is along the y direction, while it can be ignored along the x direction because the gold shell is thicker. This results in the weak dips of Fano resonance observed in the CCSNs. Concerning the peak of LSPR located at 799 nm, we can only find the strong field enhancement near the gold surface without field coupling in Fig. 4(c). It can also be found that the field intensities on the gold surface and in the dielectric core are of the same order of magnitude in Figs. 4(a) and 4(b),

thus the coupling between them can strongly affect the spectrum lineshape. But figure 4(c) shows the field intensity on the gold surface is much larger than that in the core. Thus, the Fano resonance in our proposed CCSNs originates from the strong coupling between the electric field inside the dielectric core and strong field near the gold surface.

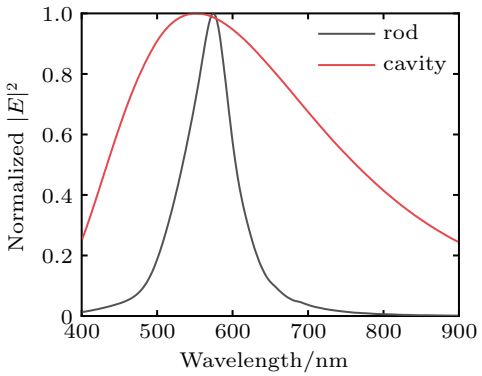


Fig. 3. The normalized electric field intensity spectra for gold nanorod and cavity.

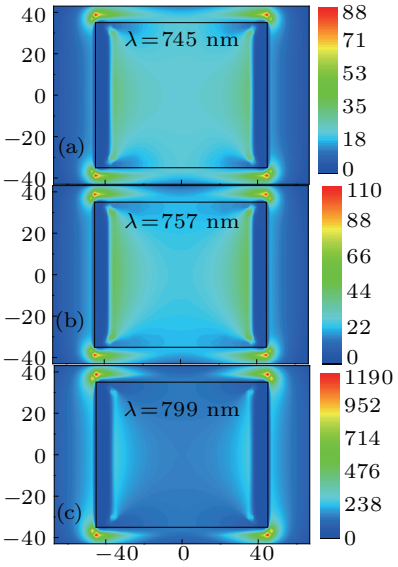


Fig. 4. Electric field intensity distributions with $\lambda = 745$ nm (a), 757 nm (b), and 799 nm (c).

We previously discussed the generation and origin of Fano resonance in the CCSNs, and found that the wavelength of Fano resonance can be adjusted just by varying the refractive index of the core. A high tuning parameter could be achieved, but the intensity of Fano resonance could not be controllednor tuned well by changing the refractive index of the core. Based on the previous results, the dependence of the intensity of Fano resonance on the polarization of the incident light is investigated in the following.

In Fig. 5, we show the extinction spectra of the CCSN with different polarized incident light. Here, we adopt the same parameters of the CCSN as those in previous discussion and fix the refractive index of core at 1.4. From Fig. 5(a) to Fig. 5(d), The polarization angle of the incident light varies from 0° to 75° as indicated in Figs. 5(a)–5(d) respectively. The black dotted line denotes the dips of Fano resonance. We can easily find that as the polarization angle of the incident light increases, the wavelength of Fano dip around 795 nm barely change. However, we can see that the intensity of Fano resonance gradually becomes weaker as the polarization angle increases. Comparing Fig. 5(a) with Fig. 5(d), we can find that the extinction cross section at Fano dip of the CCSN with 0° polarized incident light is six times higher than that with 75° polarized incident light, which means that the intensity of Fano resonance can be readily tuned by changing the polarization of the incident light. It can also be found that when the polarization angle increases to 60°, other peaks will occur. In order to illustrate these new peaks in the spectrum, we also calculate the electric field intensity distributions at 705 nm, 668 nm, and 580 nm, and the results are shown in Fig. 6. The electric quadrupole induced at 705 nm and 668 nm can be found. When we analyze the electric intensity distribution at 580 nm, we can find that an octupole mode can be generated in the system. Therefore, as the polarization angle increases, we can find some new peaks in the spectra due to the generation of higher-order modes in the system.

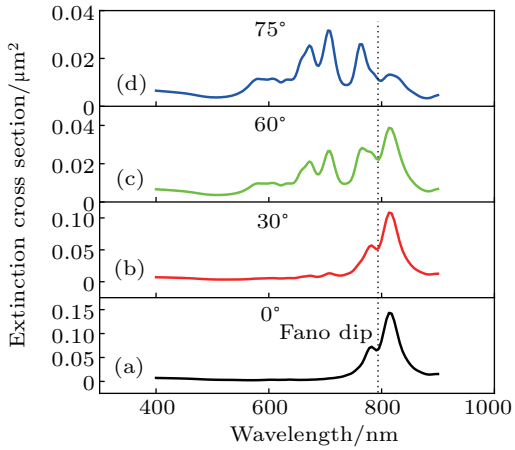


Fig. 5. Extinction cross sections of core–shell nanorod with (a) 0°, (b) 30°, (c) 60°, and (d) 75° polarized incident light, where dotted line refers to position of Fano dip and polarization angle is the angle between polarization direction of incident light and x direction.

We have discussed the tunability and origin of the Fano resonance in CCSNs, and in order to obtain a direct picture of the Fano resonance in CCSNs, the model described previously is employed. Here we choose the CCSN with the same parameters as those in previous discussion, and the refractive index of its core equals 1.3. Angle θ is set to be 0°, which means that the incident light is polarized along the x direction. In this case, this model becomes a classical two-oscillator model[11] which can be used to reproduce the response of a Fanoshell. The calculated results based on the mechanical model and the normalized extinction cross sections obtained by the FDTD simulation are shown in Figs. 7(a) and 7(b) respectively. The LSPR is modeled with wavelength $\lambda_1 = 799.6$ nm, and the

subradiant mode is modeled with wavelength $\lambda_2 = 745.5$ nm. The friction coefficient for LSPR is given by $\gamma_1 = 58.9$ THz, and that for the subradiant mode is given by $\gamma_2 = 88.3$ THz. The coupling coefficient here is assigned as $\Omega_{12} = 538.5$ THz. Comparing Fig. 7(a) and Fig. 7(b), we find the results of this model are in good agreement with the theoretical results.

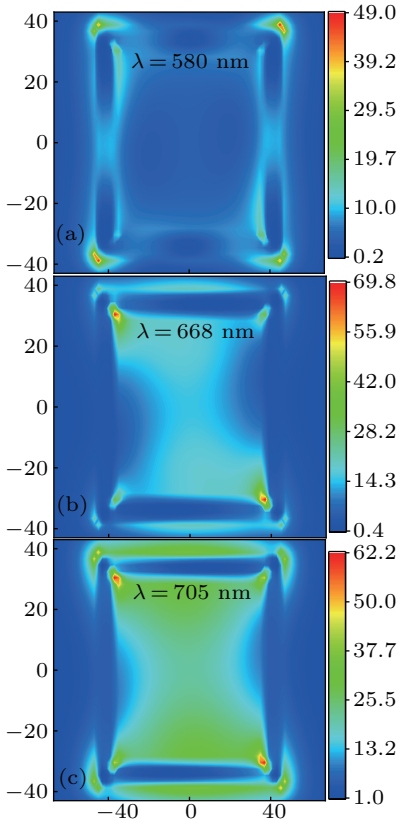


Fig. 6. Electric field intensities distribution with $\lambda = 580$ nm (a), 668 nm (b), and 705 nm (c).

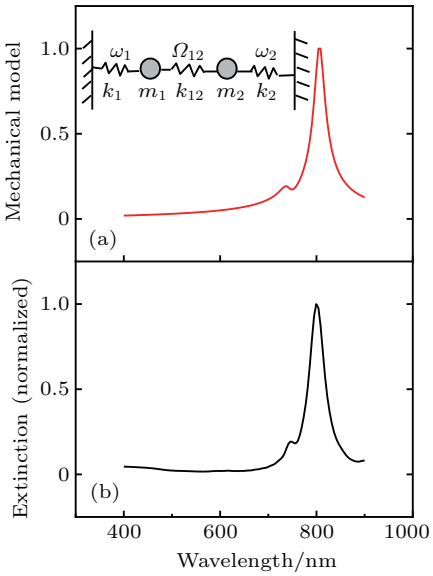


Fig. 7. (a) Results from two-oscillator model and (b) normalized extinction cross section *versus* wavelength for core–shell nanorod with $n = 1.3$.

This means the Fano resonance in CCSNs can be easily understood and analyzed by this model. The field coupling between the inner core and the out shell can be analogous to the interaction of two oscillators. Then the effect of the polarization of the incident light on Fano resonance is analyzed by this model. The refractive index of core is fixed at 1.4, and the structural parameters of the CCSN are the same as those in previous discussion. The extinction cross sections of the CCSN at the Fano dip are calculated under different-angle polarized incident light. The polarization angle of the incident light changes from 0° to 70° in steps of 10°. The results are shown in Fig. 8(a), where the extinction cross sections are all normalized by the value at $\theta = 0°$. By solving the proposed mechanical model, we can easily find that the mechanical power is a squared cosine function of the polarization angle of the incident light. Figure 8(b) shows the plot of $\cos^2(\theta)$ *versus* θ. We can find that the results in Fig. 8(a) are in agreement with those in Fig. 8(b), which means that the effect of the polarization of the incident light on the Fano resonance is dependent on $\cos^2(\theta)$, and it can be described well by this mechanical model proposed in this paper. This simple mechanical model can also be used for designing the CCSNs proposed in this paper. The field coupling can be tuned by the parameters of CCSNs and the polarization of the incident light, and the Fano resonance can be tuned by adjusting the field coupling.

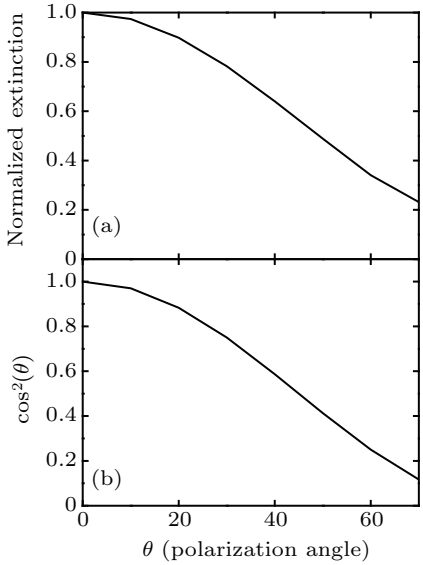


Fig. 8. (a) Normalized extinction cross section *versus* polarization angle of incident light of core–shell nanorod with $n = 1.4$ for core at Fano dip, and (b) proposed-model calculated dependence of mechanical power on polarization angle of incident light, following the square of cosine function.

4. Conclusions

In this work, we have theoretically investigated the optical extinction spectra of the proposed CCSNs, each consisting of a cylindrical dielectric core and coated thin gold film. The Fano resonance can be generated by the CCSNs, and we find that the resonance wavelength and the intensity of Fano resonance can not only be tuned, but also controlled separately

by the two independent parameters which are the refractive index of core and the polarization of the incident light that is very easy to realize. By analyzing the electric field intensity distributions, we find that the origin of Fano resonance in CCSN can be attributed to the strong field coupling of the cavity mode and near field on the gold surface. Besides, a two-oscillator mechanical model is introduced to describe the picture of Fano resonance in CCSNs. These results are helpful in understanding the generation of Fano resonance in core–shell nanostructures, and may have promising applications in biosensors and other optical nano-devices.

References

[1] Fano U 1961 *Phys. Rev.* **124** 1866
[2] Luk'yanchuk B, Zheludev N I, Maier S A, Halas N J, Nordlander P, Giessen H and Chong C T 2010 *Nat. Mater.* **9** 707
[3] Mirin N J, Bao K and Norlander P 2009 *J. Phys. Chem. A* **113** 4028
[4] Verellen N 2009 *Nano Lett.* **9** 1663
[5] Bao Y J, Peng R W, Shu D J, Wang M, Lu X, Shao J, Lu W and Ming N B 2008 *Phys. Rev. Lett.* **101** 087401
[6] Qin L, Zhang K, Peng R W, Xiong X, Zhang W, Huang X R and Wang M 2013 *Phys. Rev. B* **87** 125136
[7] Bao K, Mirin N A and Nordlander P 2010 *Appl. Phys. A* **100** 333
[8] Niu L, Zhang J B, Fu Y H, Kulkarni S and Luky'anchuk B 2011 *Opt. Express* **19** 22974
[9] Lassiter J B, Sobhani H, Knight M W, Mielczarek W S, Nordlander P and Halas N J 2012 *Nano Lett.* **12** 1058
[10] Ye J, Wen F, Sobhani H, Lassiter J B, Dorpe P V, Nordlander P and Halas N J 2012 *Nano Lett.* **12** 1660
[11] Mukherjee S, Sobhani H, Lassiter J B, Bardhan R, Nordlander P and Halas N J 2010 *Nano Lett.* **10** 2694
[12] Li Y, Zhong F, Ding P, Chen Z, Luo F, Shao L, Du Y, Chen L and Lei M 2019 *Nanotechnology* **30** 375401
[13] Wu X, Dou C, Xu W, Zhang G, Tian R and Liu H 2019 *Chin. Phys. B* **28** 014204
[14] Lovera A, Gallinet B, Nordlander P and Martin O J F 2013 *ACS Nano* **7** 4527
[15] Fan S H and Joannopoulos J D 2002 *Phys. Rev. B* **65** 235112
[16] Fan S H, Suh W and Joannopouls J D 2003 *J. Opt. Soc. Am. A* **20** 569
[17] Lee K L, Wu S H, Lee C W and Wei P K 2011 *Opt. Express* **19** 24530
[18] King N S, Liu L, Yang X, Cerjan B, Everitt H O, Nordlander P and Halas N J 2015 *ACS Nano* **9** 10628
[19] Thyagarajan K, Butet J and Martin O J F 2013 *Nano Lett.* **13** 1847
[20] Fan J A, Wu C, Bao K, Bao J M, Bardhan R, Halas N J, Manoharan V N, Nordlander P, Shvets G and Capasso F 2010 *Science* **328** 1135
[21] Jia Z Y, Li J N, Wu H W, Wang C, Chen T Y, Peng R W and Wang M 2016 *J. Appl. Phys.* **119** 074302
[22] Averitt R D, Sarkar D and Halas N J 1997 *Phys. Rev. Lett.* **78** 4217
[23] Mock J J, Barbic M, Smith D R, Schultz D A and Schultz S 2002 *J. Chem. Phys.* **116** 6755
[24] Lassiter J B, H Sobhani H, Fan J A, Kundu J, Capasso F, Nordlander P and N J Halas N J 2010 *Nano Lett.* **10** 3184
[25] Huang M, Chen D, Zhang L and Zhou J 2016 *Chin. Phys. B* **25** 057303
[26] Mousavi S H, Kholmanov I, Alici K B, Purtseladze D, Arju N, Tatar K, Fozdar D Y, Suk J W, Hao Y, Khanikaev A B, Ruoff R S and Shvets G 2013 *Nano Lett.* **13** 1111
[27] Cao T, Wei C, Simpson R E, Zhang L and Cryan M J 2015 *Sci. Rep.* **4** 4463
[28] Hao F, Nordlander P, Sonnerfraud Y, Dorpe P V and Maier S A 2009 *ACS Nano* **3** 643
[29] Zhong H H, Zhou J H, Gu C J, Wang M, Fang Y T, Xu T and Zhou J 2017 *Chin. Phys. B* **26** 127301
[30] Prodan E, Radloff C, Halas N J and Nordlander P 2003 *Science* **302** 419